NAMVS 2021 – Tukkaraja (Ed.)

Airflow characteristic curves for a mature block cave mine

R. Bhargava, P. Tukkaraja, A. Adhikari & S.J. Sridharan
South Dakota School of Mines and Technology, Rapid City, SD, USA

V.V.S. Vytla
MSC Software, USA

ABSTRACT: Block/panel caving is an underground bulk mining method that utilizes gravitational force for mining massive, steeply dipping and deep-seated ore deposits at a lower operating cost. Since caving is a dynamic process, the design of an effective ventilation system is a challenging task and therefore, estimation of airflow resistance offered by the broken rock inside the cave is critical. The complex and dynamic nature of caving also makes it difficult to predict the airflow resistance by using traditional approaches. This study investigates the effect of changes in the bulk porosity of the broken rock on the cave airflow resistance using Computational Fluid Dynamics (CFD) approach. The results show an inverse relationship between the cave airflow resistance and the bulk cave porosity.

Keywords: Porosity, Cave airflow resistance, Panel/Block cave mining, flow through porous media

1 INTRODUCTION

Mass mining methods such as block/panel caving tend to be an ideal choice for massive, steeply dipping and deep-seated ore deposits with an ability to extract deposits at high production rates and low operating costs. The deposits mined by the caving mining method are generally disseminated or low grade in nature [1]. Previous studies reported the advantage of block/panel caving mining method in terms of the maximization of net present value for low-grade ore deposits [2]. Thus, the economics for a low-grade ore deposit also tend to tilt in favor of block/panel caving. An optimally designed block/panel cave mining method can have the lowest operating cost as compared to other underground mining methods subject to conditions of keeping ore dilution under checked limits [3, 4]. Super caves have been defined as those underground cave mines which have a production rate exceeding 25 Mt per annum or approximately 70 kt/day [5, 6]. The evolution of production rates over years with respect to conventional and super caves is shown in Figure 1.

The cave mining methods demands a robust ventilation system to support the high production rates of the future super caves. Therefore, this research study contributes to the knowledge base of block/panel cave mine ventilation. This study investigates a less explored concept of cave airflow resistance that plays an important role in the ventilation system with regards to requirements of air quantity.

DOI: 10.1201/9781003188476-6

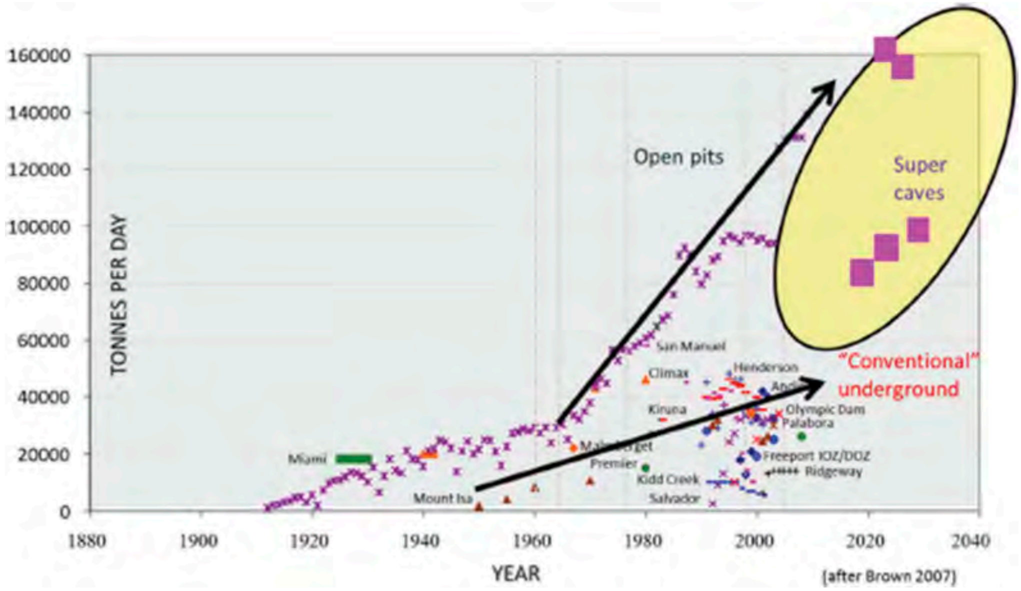

Figure 1. Production rates: Open pits, conventional underground mining & super caves [5, 6].

2 LITERATURE REVIEW

In panel caving, the cave is assumed to be fully developed when the broken rock reaches the economical ore boundary. Airflow resistance of a cave is defined as the resistance offered by the broken rock pile to the airflow when airflows through the rock pile inside the cave. The porosity of the rockpile is defined as the percentage of air/void space inside the total volume occupied by the rock pile. The porosity of a cave varies as the cave propagates; it plays an important role to buffer an air blast event. Thus, porosity and the broken rock resistance are important parameters for modeling airflow inside the cave [7]. Leakage of airflow into the cave and ore passes from the production drifts is also an important phenomenon; it has been mentioned that around 40 percent of air supplied into the production drifts leaks into the cave and the ore passes, so the production drift airflow quantity should be adjusted for accounting these leakages [8].

Several attempts have been made in the past for characterizing airflow through broken rock [9, 10]. Porous media can be modeled as a discrete or continuum model. Discrete modeling offers certain advantages over the continuum model with regards to accuracy and realistic approach but the meshing of the geometry becomes a tedious task in discrete modeling. The advantage of the continuum model is that it is computationally inexpensive but accuracy gets sacrificed in the process [11]. CFD modeling has been successfully used in the past for underground mining applications involving gob characteristics for a longwall gob involving spontaneous heating and airflow patterns in bord and pillar mining [12, 13]. In a multi-lift caving operation, the older working areas might be connected to a mature cave[11]. Attempts for predicting the airflow resistance of a mature panel cave have also been made in the past with limited success. The previous study did not consider the connection of the cave to the older workings which is very unlikely for a mature cave although the study indicated that the flow inside the cave is neither laminar nor turbulent [11].

3 MODEL LAYOUT AND RESEARCH APPROACH

This study considered a panel cave continuum model with a cave dimension 375 m x 256 m x 356 m (height x length x width) and nine production drifts, three undercut inlet ducts, eight undercut drifts, eight exhaust drifts. The model also includes 94 drawbells, broken rock region and uncaved in-situ rock inside the cave. These regions are simulated as porous zones. The isometric, side and front views of the panel cave model are shown in Figures 2 and 3. The cave advancement direction is assumed from right to left. Each of the production drifts, undercut drifts and exhaust drifts have dimensions of 4.3 m x 4.3 m. There are three undercut inlet ducts (inside the undercut drifts) of size 1 m x 1 m and are used for ventilating undercut drifts. The computational time has been kept in mind while modeling the airflow through cave zones. Therefore, broken rock zones and in-situ waste rock zones are modeled diagonally in the model consisting of 16 broken rock zones and 2 uncaved in-situ waste rock zones. Each broken rock zone is divided into 3 subregions laterally to conform to the observation in the field that the boundary of the cave has higher porosity values with larger particle sizes as compared to the mid-region. Sub-regions for broken rock zone 10 are shown as an example in Figure 3. The bulk cave porosity is calculated by dividing the sum of the porous volume of broken rock from all the regions by the total volume of the cave (excluding intact rock zone).

This study modeled broken rock zones as porous media. The methodology used for this study is shown in Figure 4. Different scenarios of cave resistance are simulated by changing

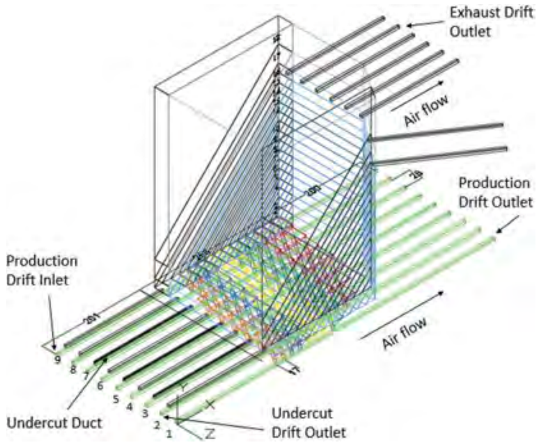

Figure 2. Isometric view of panel cave model [14].

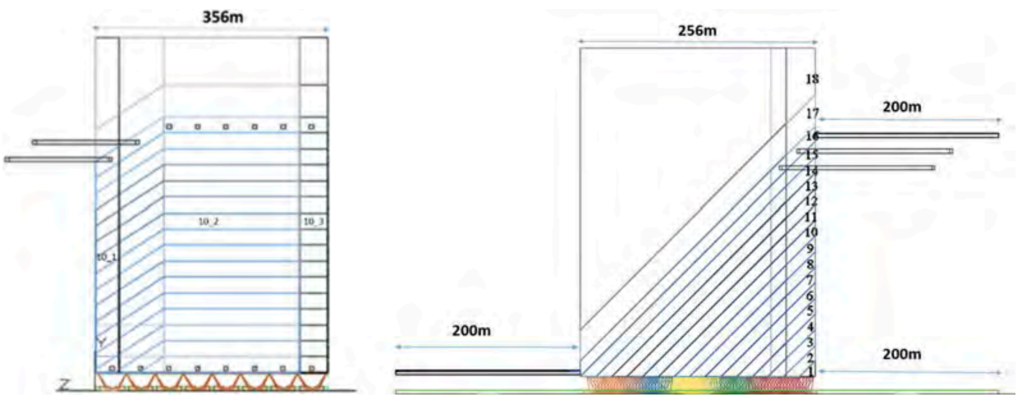

Figure 3. Side and front view of panel cave model [14].

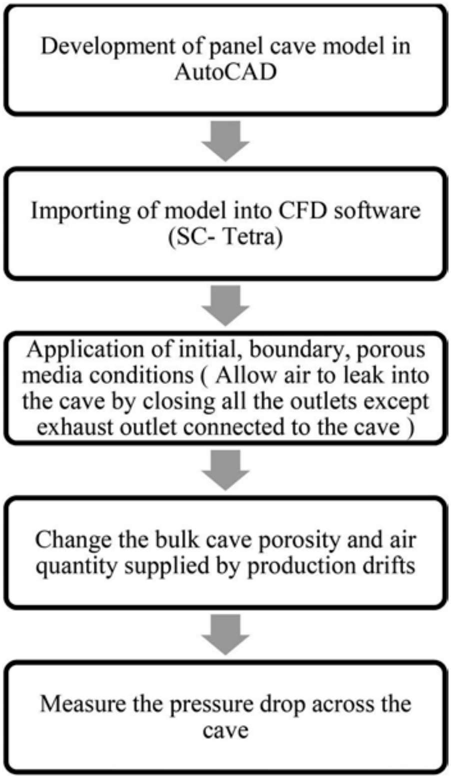

Figure 4. Airflow resistance calculation methodology.

cave porosity values in the model, and the pressure loss (the pressure difference is measured across the cave) obtained from the CFD analysis is plotted against airflow to obtain the equation for airflow resistance under different porosity conditions. The pressure difference is measured across the cave. Figure 5 shows the schematic of air leaking into the cave while all the outlets except the exhaust outlet have been closed to calculate the airflow resistance by allowing the air to leak through porous media of broken rock. The undercuts have not been considered in this study for calculating the airflow resistance as their effect would be minimal for a mature panel cave. This study considers that the matured cave is connected to old workings through the exhaust drifts in the model.

A reliable result from the CFD model is highly dependent on the boundary conditions applied to the model. A summary of boundary conditions applied to the panel model is presented in Table 1. Static pressure condition is applied to the exhaust drift outlet. Natural inflow/outflow condition is used for the rooftop. This condition assumes that velocity and pressure do not change in the normal direction. It is used because the flow is assumed to continue into other sections of the mine [15].

SC/Tetra (CFD software program) consists of three sets of programs. These include the pre-processor (for creation of computational mesh and setting the boundary conditions for the simulation), solver (for the execution of analysis) and post-processor (for visualization and analyze the results). The simulation study considers a steady-state incompressible and turbulent airflow through the panel cave model. Standard k-ε turbulence model is used for the study to consider the effects of turbulence [16]. Flow field can be obtained by solving momentum and mass conservation equations. Therefore, for obtaining velocity and pressure

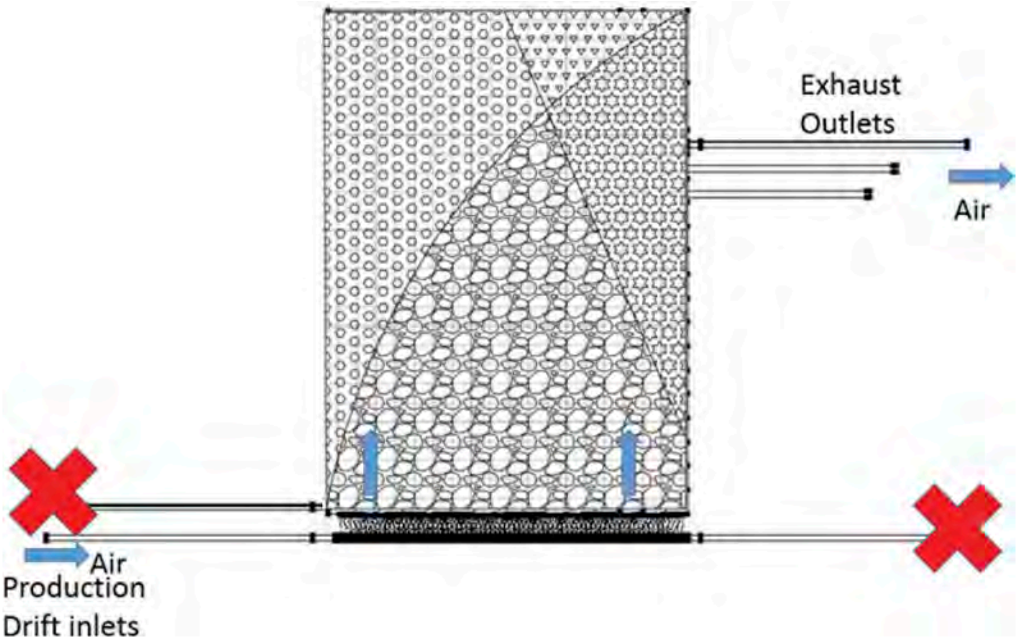

Figure 5. Schematic of air leaking into the cave.

Table 1. Boundary conditions.

Region	Boundary Condition Type	Value/Condition
Production Drifts (9 Nos.)	Fixed velocity	0.75 m/s, 1 m/s, 1.25 m/s, 1.5 m/s and 1.75 m/s
Undercut inlet Drift duct (3 Nos.)	Wall condition	n/a
Undercut Drift (8 Nos.)	Wall condition	n/a
Exhaust Drift (8 Nos.)	Static Pressure	zero Pa
Roof Top	Outlet	Natural inflow/outflow

fields, momentum and mass conservation equations have been solved respectively. A porous media condition is also used to consider the pressure drop of flow through the broken rock [17].

For obtaining reliable results from the CFD simulations, it is also important that the simulation results are grid-independent. Mesh independent study was also conducted for the mature panel cave model. From the analysis of the results with mesh elements ranging from 5.5 million to 15.8 million, it was observed that a further increase in the mesh elements from 11.8 million did not have a significant effect on the results. Hence, 11.8 million mesh elements were used for this study.

4 RESULTS AND ANALYSIS

For calculating the airflow resistance of the broken rock, the mature panel cave model was analyzed under six different bulk cave porosities and five different air quantities through the production drift. Figure 6 represents the measurement of airflow pressure at

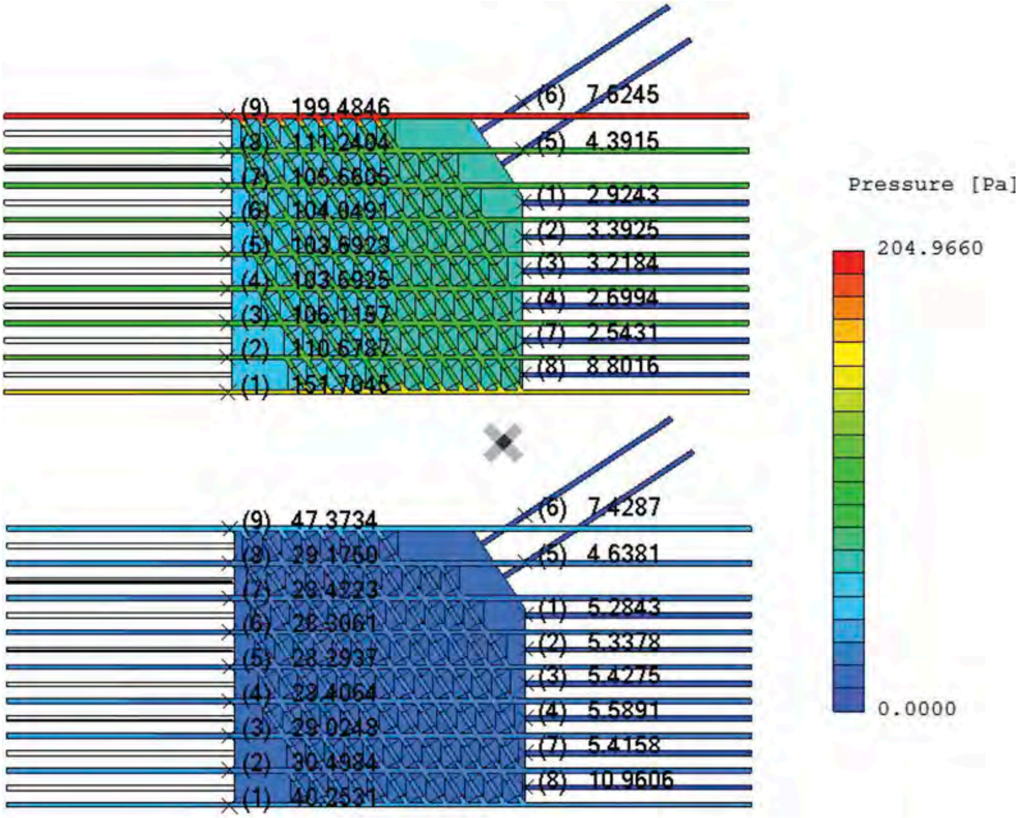

Figure 6. Pressure measurement at entry and exit of the cave in the production and exhaust drifts at 35% and 56% cave porosity condition (top to bottom).

the entry of the cave inside the production drifts and at the exit of the cave inside the exhaust drifts for cave porosities of 35 and 56 % and an airflow rate of 291 m^3/s in the production drifts.

For a given porosity of the cave and airflow in the production drifts, the pressure difference across the cave is calculated and then plotted against the airflow quantity flowing through the cave as shown in Figure 7. For example, for a bulk cave porosity of 35 %, five different air quantities were simulated. Therefore, for six different bulk cave porosities, a total of 30 simulations were performed to develop the pressure-quantity (P-Q) characteristic curves for a mature panel cave mine. Figure 8 shows the variation of the airflow resistance value with respect to the bulk cave porosity; these values are tabulated in Table 2.

From Figure 7, the relationship between the pressure difference (Pa) across the cave and the airflow resistance (Ns^a/m^b), quantity supplied (m^3/s) can be summarized by

$$\Delta P = R\ Q^c \tag{1}$$

where, $1.8 \leq a \leq 1.9,\ 7.4 \leq b \leq 7.7\ \mathit{and}\ 1.8 \leq c \leq 1.9$

Equation 1 suggests that the flow inside the cave is neither fully laminar nor fully turbulent.

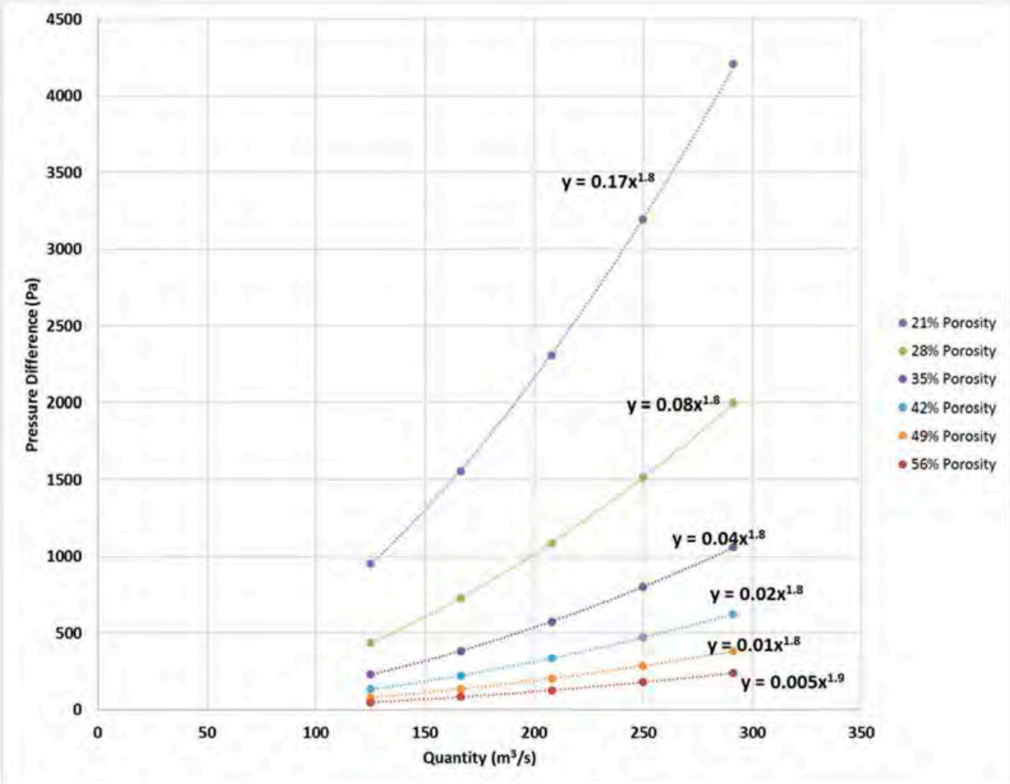

Figure 7. Pressure-Quantity characteristic curves.

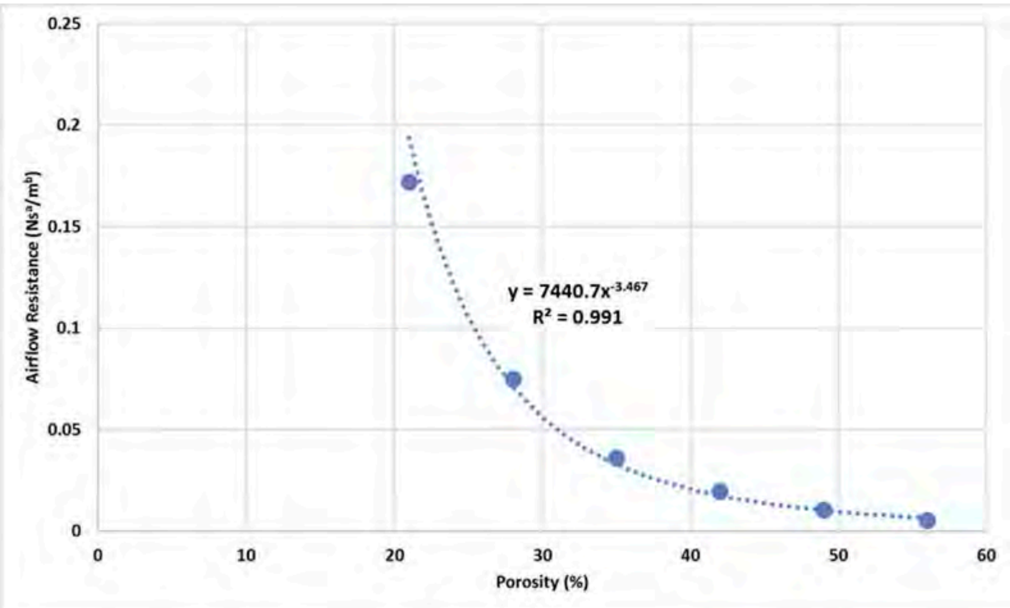

Figure 8. Airflow resistance vs. bulk cave porosity.

Table 2. Cave porosity and airflow resistance.

Cave Porosity (%)	Cave Airflow Resistance (Ns^a/m^b)
21	0.17
28	0.08
35	0.04
42	0.02
49	0.01
56	0.005

5 CONCLUSIONS

The airflow characteristics of a block cave mine is examined with the help of CFD using a continuum approach. This study reveals that porosity plays an important role in changing the resistance offered by the broken rock to the airflow leaking into the cave. The airflow resistance increases as the porosity of the broken rock pile decreases. The pressure-quantity relationship for the airflow through the broken rock is different from the Atkinson's law for the turbulent flow in a regular mine airway. The resistance of the block cave mine changes dynamically with the bulk porosity of the broken rock. This study is valid for a mature panel cave (with no air gap) where the cave is connected to the older working areas.

ACKNOWLEDGMENTS

The authors acknowledge the financial support from the National Institute for Occupational Safety and Health (NIOSH) (200-2014-59613) for conducting this research.

REFERENCES

1. Lovejoy, C., *Block caving: Keeping up with caving*. Mining magazine, 2012(6): p. 46–64.
2. Lei, Q., et al., *Effects of geomechanical changes on the validity of a discrete fracture network representation of a realistic two-dimensional fractured rock*. International journal of rock mechanics and mining sciences, 2014. **70**: p. 507–523.
3. Laubscher, D., *Cave mining-the state of the art*. Journal of The Southern African Institute of Mining and Metallurgy, 1994. **94**(10): p. 279–293.
4. Trueman, R., R. Castro, and A. Halim, *Study of multiple draw-zone interaction in block caving mines by means of a large 3D physical model*. International Journal of Rock Mechanics and Mining Sciences, 2008. **45**(7): p. 1044–1051.
5. Brown, E., *Block Caving Geomechanics. 2nd edn*. The International Caving Study, 2007.
6. C deWolfe and I. Ross. *Super caves - benefits, considerations and risks*. in *Proceedings of the 7th International conference and exhibition on mass mining, Sydney*. 2016.
7. Vejrazka, C., *Northparkes Mines' Current Air Blast Risk Assessment Practices for Block Caving Operations*. 2016.
8. Brokering, R.D., D.M. Loring, and C.J. Rutter. *Practical Implementation of VOD at the Henderson Mine*. in *16th North American Mine Ventilation Symposium*. 2017. Golden, Colorado.
9. Schafrik, S., *The use of packed sphere modelling for airflow and heat exchange analysis in broken or fragmented rock*. 2015, Laurentian University of Sudbury.
10. Schafrik, S. and D.L. Millar, *Verification of a CFD code use for air flow simulations of fractured and broken rock*. Applied Thermal Engineering, 2015. **90**: p. 1131–1143.
11. Baysal, A., et al. *Prediction of Airflow Resistance of a Matured Panel cave*. in *16th North American Mine Ventilation Symposium*. 2017. Golden.
12. Yuan, L. and A. Smith. *Effects of ventilation and gob characteristics on spontaneous heating in longwall gob areas*. in *of: Proceedings of the 12th US/North American Mine Ventilation Symposium*. 2008.

13. Ranjan, M. and S.K. Karan Kumar, *Mine ventilation in a bord and pillar mines using CFD*. 2013.
14. Bhargava, R., et al. *CFD Analysis of the Effect of Porosity, Quantity and Emanating Power Variation on Gas Emissions in Block/Panel Cave Mines*. in *11th International Mine Ventilation Congress*. 2019. China.
15. Ajayi, K., et al., *Computational Fluid Dynamics Study of Radon Gas Migration in a Block Caving Mine*. 15th North American Mine Ventilation Symposium, 2015: p. 341–348.
16. Hurtado, J.P., et al., *Shock losses characterization of ventilation circuits for block caving production levels*. Tunnelling and underground space technology, 2014. **41**: p. 88–94.
17. Cradle, *User's Guide: Basics of CFD Analysis. 2015*.

PROCEEDINGS OF THE 18TH NORTH AMERICAN MINE VENTILATION SYMPOSIUM (NAMVS 2021), JUNE 12-17, 2021, RAPID CITY, SOUTH DAKOTA, USA

Mine Ventilation

Editor

Purushotham Tukkaraja, Ph.D., QP

Mining Engineering & Management, South Dakota Mines, Rapid City, SD, USA

CRC Press
Taylor & Francis Group
Boca Raton London New York

CRC Press is an imprint of the
Taylor & Francis Group, an **informa** business
A BALKEMA BOOK

CRC Press/Balkema is an imprint of the Taylor & Francis Group, an informa business

Typeset by Integra Software Services Pvt. Ltd., Pondicherry, India

Library of Congress Cataloging-in-Publication Data

A catalog record has been requested for this book

Published by: CRC Press/Balkema
Schipholweg 107C, 2316 XC Leiden, The Netherlands
e-mail: enquiries@taylorandfrancis.com
www.routledge.com – www.taylorandfrancis.com

ISBN: 978-1-032-03679-3 (Hbk)
ISBN: 978-1-032-03681-6 (Pbk)
ISBN: 978-1-003-18847-6 (eBook)
DOI: 10.1201/9781003188476